


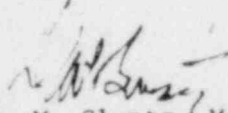
NEDO-24288  
80NED299  
Class I  
February 1981

MARK II CONTAINMENT PROGRAM

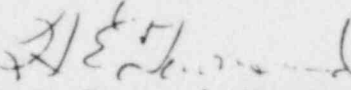
GENERIC CONDENSATION OSCILLATION LOAD  
DEFINITION REPORT

Reviewed:   
G. E. Wade, Manager  
Mark I/II Containment Engineering

Reviewed:   
R. J. Muzzo, Manager  
Mark II Containment Design

Reviewed:   
D. M. Gluntz, Manager  
Containment Experiments

Approved:   
R. W. Zanni, Manager  
Containment Design

Approved:   
H. E. Townsend, Manager  
Containment Technology

NUCLEAR POWER SYSTEMS DIVISION • GENERAL ELECTRIC COMPANY  
SAN JOSE, CALIFORNIA 95125

GENERAL  ELECTRIC

8103180588

#### DISCLAIMER OF RESPONSIBILITY

The only undertakings of the General Electric Company respecting information in this document are contained in the contracts for Mark II Containment Consulting Services between the General Electric Company and each of the members of the U.S. Mark II Owners Group, effective variously June 9, 1975, June 13, 1975, or July 29, 1975, and nothing contained in this document shall be construed as changing the contracts. The use of this information by anyone other than the members of the U.S. Mark II Owners Group either themselves or through their technical consultants, or for any purpose other than that for which it is intended under the contracts, is not authorized; and with respect to any unauthorized use, the General Electric Company makes no representation or warranty, express or implied, and assumes no liability of any kind as to the completeness, accuracy, usefulness or non-infringing nature of the information contained in this document.

## CONTENTS

	<u>Page</u>
ABSTRACT	xi
1. INTRODUCTION	1-1
2. DEFINITION AND APPLICATION OF LOAD	2-1
2.1 Basic CO Load	2-1
2.1.1 Description of Load Case	2-1
2.1.2 Criteria for Selection of 4TCO Data	2-1
2.1.3 Description of Data Selected	2-1
2.2 CO Load for Combination with ADS	2-2
2.2.1 Description of Load Case	2-2
2.2.2 Criteria for Selection of 4TCO Data	2-4
2.2.3 Description of Data Selected	2-5
2.3 Application Procedure	2-5
2.3.1 Spatial Distribution of Applied Pressure	2-5
2.3.2 Conditions for Load Cases	2-6
3. JUSTIFICATION OF LOAD DEFINITION	3-1
3.1 Comparison of Mark II and 4TCO Blowdown Conditions	3-1
3.1.1 Methodology for Best-Estimate Predictions	3-1
3.1.2 Mark II and 4TCO Blowdown Calculations	3-2
3.1.3 Mark II Versus 4TCO Conditions Comparison	3-3
3.1.4 Plant Unique Adjustments for Pool Temperature	3-3
3.2 Comparison of Mark II Containment and 4TCO Geometries	3-4
3.2.1 Break Area Per Vent	3-4
3.2.2 Vent Length	3-4
3.2.3 Vent Submergence	3-5
3.2.4 Vent to Pool Bottom Clearances	3-5
3.2.5 Pool Area-to-Vent Area Ratio	3-5
3.2.6 Drywell Volume Per Vent	3-5
3.2.7 Wetwell Airspace Volume-to-Drywell Volume Ratio	3-6
3.2.8 Pool Mass Per Vent	3-6
3.2.9 Plant Unique Adjustments for Pool Geometry	3-6
3.3 4TCO Comparison With Multivent Data	3-6
3.3.1 Comparison of JAERI and 4TCO Suppression Pool Pressures	3-8
3.3.2 Comparison of JAERI and 4TCO Drywell Pressures	3-9
3.4 4TCO Fluid-Structure Interaction Evaluations	3-9
3.4.1 Acoustic Modes	3-10
3.4.2 Facility Bounce Mode	3-12
3.4.3 Baseplate/Sidewall Vibration	3-13
4. CONCLUSION	4-1
REFERENCES	R-1

CONTENTS (Continued)

	<u>Page</u>
APPENDICES	
A. AMPLIFIED-RESPONSE-SPECTRA CONFIRMATION OF SELECTED TIME PERIODS	A-1
B. PLANT UNIQUE ASSESSMENT OF THE 4TCO DATA FOR LASALLE	B-1



## TABLES

<u>Table</u>	<u>Title</u>	<u>Page</u>
2-1	4TCO Time Periods for Basic CO Load and CO Load with ADS	2-7
2-2	Bases and Assumptions for the ADS Event	2-8
3-1	4TCO versus Mark II Geometric Parameters	3-15
3-2	Initial Conditions for Comparable JAERI and 4TCO Tests	3-16
3-3	Average rms Pressure Values at Vent Exit and Pool Bottom	3-17

## ILLUSTRATIONS

<u>Figure</u>	<u>Title</u>	<u>Page</u>
2-1	Envelope of PSD Values Observed for CO in 4TCO Tests	
2-2	Wetwell Bottom Center Pressure Time History, 4TCO Run 15, 39 to 41 Seconds	
2-3	Drywell Pressure Time History, 4TCO Run 15, 39 to 41 Seconds	
2-4	Wetwell Bottom Center Pressure Time History, 4TCO Run 22, 13 to 15 Seconds	
2-5	Drywell Pressure Time History, 4TCO Run 22, 13 to 15 Seconds	
2-6	PSD - Wetwell Bottom Center Pressure for 4TCO Run 15, 39 to 41 Seconds	
2-7	PSD - Wetwell Bottom Center Pressure for 4TCO Run 22, 13 to 15 Seconds	
2-8	Mass Flux and Bulk Pool Temperature at CO-to-Chugging Transition in 4TCO Runs	
2-9	Mark II Maximum Mass Flux at ADS versus CO-to-Chugging Transition in 4TCO Tests	
2-10	Spatial Distribution of CO Load	2-10
2-11	Basic CO Load - Range of Conditions	
2-12	CO Load with ADS - Range of Conditions	
3-1	Steam Generator Dome Pressure - Measured versus Predictions - 4TCO Run 3	
3-2	Steam Generator Dome Pressure - Measured versus Predictions - 4TCO Run 2	
3-3	Steam Generator Dome Pressure - Measured versus Predictions - 4TCO Run 12	
3-4	Vent Air Content - Measured versus Prediction - 4TCO Run 8	
3-5	Vent Air Content - Measured versus Prediction - 4TCO Run 9	
3-6	Vent Air Content - Measured versus Prediction - 4TCO Run 12	
3-7	Mark II Plants Calculated Blowdown Conditions - Vent Steam Mass Flux versus Bulk Pool Temperature	

## ILLUSTRATIONS (Continued)

<u>Figure</u>	<u>Title</u>	<u>Page</u>
3-8	Mark II Plants Calculated Blowdown Conditions - Vent Steam Mass Flux versus Vent Air Content	
3-9	4TCO Calculated Blowdown Conditions - Vent Steam Mass Flux versus Bulk Pool Temperature	
3-10	4TCO Calculated Blowdown Conditions - Vent Steam Mass Flux versus Vent Air Content	
3-11	Mark II Plants and 4TCO Comparison on Map of Vent Steam Mass Flux versus Bulk Pool Temperature	
3-12	Mark II Plants and 4TCO Comparison on Map of Vent Steam Mass Flux versus Vent Air Content	
3-13	JAERI and 4TCO Bulk Pool Temperature Comparison	
3-14	Pool Bottom rms Pressure Time Histories, JAERI Test 1101	
3-15	Pool Bottom rms Pressure Time Histories, 4TCO Runs 2, 5 and 7	
3-16	Pool Bottom rms Pressure Time Histories, 4TCO Runs 26 and 28	
3-17	Pool Bottom rms Pressure Time History, 4TCO Run 25	
3-18	Bounding PSD for 4TCO Runs 2, 5 and 7	
3-19	Bounding PSD for 4TCO Runs 26 and 28	
3-20	Bounding PSD for 4TCO Run 25	
3-21	Bounding PSD for JAERI Test 1101	
3-22	Comparison of Bounding Drywell Pressure PSD for Comparable 4TCO Runs with JAERI Test 1101	
3-23	PSD of Downcomer Exit Pressure for 4TCO Run 15, 30 to 40 Second Period	
3-24	PSD of Downcomer Exit Pressure for 4TCO Run 15, 40 to 50 Second Period	
3-25	Ratio of Bottom Center to Downcomer Exit Pressure Amplitude for 4TCO Run 15, 30 to 40 Second Period	
3-26	Ratio of Bottom Center to Downcomer Exit Pressure Amplitude for 4TCO Run 15, 40 to 50 Second Period	

## ILLUSTRATIONS (Continued)

<u>Figure</u>	<u>Title</u>	<u>Page</u>
3-27	Baseplate Flange Accelerometer Reading for 4TCO Run 9, 16 to 18 Second Period	
3-28	PSD of Pressure at 12-ft Elevation, 315° Orientation for 4TCO Run 15, 40 to 42 Second Period	
3-29	PSD of Pressure at 12-ft Elevation, 45° Orientation for 4TCO Run 15, 40 to 42 Second Period	
3-30	Calculated Ratio of Flexible to Rigid Wall Pressure Amplitude for Unit Harmonic Acceleration at Vent Exit	
3-31	Ratio of Hoop Strain to Pressure Amplitude at 12-ft Elevation for 4TCO Run 15, 40 to 50 Second Period	

## ABSTRACT

*This document defines the generic condensation oscillation (CO) load for the Mark II pressure suppression containments. This load definition is based on direct application of pressure measurements in the drywell and suppression pool from the full-scale single-vent 4TCO tests. Two load cases, the basic CO load and a low amplitude CO load, are presented in this report. The first load case covers all LOCA blowdown conditions resulting in CO, except for those at which the Automatic Depressurization System (ADS) may be actuated. The second load case is presented specifically for combination with ADS. This load is based on the small liquid break tests and low mass flux conditions that are representative of conditions at the time of ADS actuation. The 4TCO data used for these two load cases have not been adjusted to take credit for reductions due to multi-vent or fluid-structure interaction effects.*

1. INTRODUCTION

The latest series of tests in the 4T Pressure Suppression Test Facility (Reference 1) was conducted to investigate the condensation oscillation (CO) phenomena and demonstrate that the previous CO load definition described in Mark II Containment Dynamic Forcing Function Information Report (DFFR) Rev. 3 (Reference 2) was conservative. These tests are referred to as the 4TCO tests. The data evaluations performed as described in Reference 1 suggest that the DFFR load definition is not bounding at all frequencies. Consequently, a Mark II generic load definition program was undertaken to define a CO load based on the 4TCO test data.

The approach taken on this Mark II generic CO load definition is a direct application of 4TCO data. Two CO load cases are presented in this report. The first load is the basic CO load. It is a bounding representation of the CO loading that may occur during a Mark II Loss-of-Coolant Accident (LOCA). The second load is for the combination of loads resulting from CO and actuation of the Automatic Depressurization System (ADS).

The basic CO load bounding time intervals were selected on the basis of power by frequency analysis of the pool bottom pressure from the entire 4TCO data base for CO. The pool bottom and drywell pressure time histories corresponding to these bounding time intervals are to be applied directly as rigid wall loads to the containment structural models. Fluid-structure interaction (FSI) evaluations and studies of available full-scale multivalent CO test data were performed to confirm the conservatism of this approach.

Although there is some uncertainty whether the CO with ADS load combination exists for all Mark II plants, the conservative approach taken here was to accept the combination and define a separate CO load for this combination. This CO load for combination with ADS was also defined on the basis of the 4TCO data. However, the data base for this load was limited to time periods with low vent mass fluxes from the small liquid break tests that are most



representative of Mark II plant conditions with ADS actuation. This load can be used for combinations other than CO with ADS provided it can be shown that the criteria used for selection of this data base are applicable for the other combinations.

## 2. DEFINITION AND APPLICATION OF LOAD

### 2.1 BASIC CO LOAD

#### 2.1.1 Description of Load Case

The basic CO load case is a bounding load for any CO condition expected during a hypothetical LOCA in a Mark II plant.

The basic CO load is a generic load applicable to all domestic Mark II plants. The basic CO load is composed of a group of pressure time histories from the test data obtained during the 4TCO test program (Reference 1). The test data used are the suppression pool pressure (bottom center pressure) measurements and the drywell acoustic pressure measurements.

#### 2.1.2 Criteria for Selection of 4TCO Data

All 28 of the 4TCO test runs were analyzed to determine the bounding time periods. The criteria for the selection of these time periods was to bound the maximum power spectral density (PSD) values observed in the bottom center pressure (BCP) throughout the CO period in all runs, in any 2.043 second block for all frequencies from 0 through 60 Hz, in approximately 0.5 Hz increments. The selected time periods were independently confirmed to be bounding by the amplified-response-spectra analysis as described in Appendix A.

#### 2.1.3 Description of Data Selected

Figure 2-1 shows the envelope of the PSD values for the BCP for the entire CO period for all 4TCO runs. The specific 4TCO runs that contribute to this envelope are also shown in this same figure. The time periods corresponding to the maximum PSD values for these runs which comprise the basic CO load are listed in Table 2-1. Figures 2-2 through 2-5 are samples of the BCP and drywell pressure time histories for two of the time periods included in the basic CO load definition. Figures 2-6 and 2-7 show the corresponding PSD plots for Figures 2-2 and 2-4.

## 2.2 CO LOAD FOR COMBINATION WITH ADS

### 2.2.1 Description o Load Case

The ADS, an intergral part of the Emergency Core Cooling System, is a protection system that rapidly depressurizes the reactor pressure vessel for certain break sizes less than the Design Basis Accident (DBA). The ADS operation depressurizes the reactor pressure vessel permitting the operation of the low pressure cooling systems which will maintain the water level in the reactor pressure vessel. The ADS typically consists of a group of safety relief valves that will open with coincident high drywell pressure and low reactor water level signals and subsequent 90 to 120 second delay. This actuation of the ADS when there is vent blowdown flow into the suppression pool may lead to the simultaneous occurrences of loadings on the containment boundary due to the safety relief valve discharge and condensation at the vent exit.

An investigation was conducted to determine if the vent blowdown conditions concurrent with ADS could result in CO phenomena, and to define the CO load magnitude for combination with the ADS load if the CO plus ADS load combination could not be ruled out. This study included (1) evaluating the 4TCO test data to define the CO-to-chugging transition conditions, (2) calculating the vent blowdown conditions at the time of ADS actuation, and (3) comparing the plant calculated vent blowdown conditions at ADS actuation with CO-to-chugging transition conditions.

#### 2.2.1.1 CO-to-Chugging Transition Conditions

The distinguishing feature between CO and chugging is the character of the steam condensation process at the vent exit. During CO the wall pressure oscillations are nearly continuous with the steam/water interface always outside the vent exit. During chugging the condensation takes place in short duration events (called chugs) which are intermittent in nature and associated with re-entry of water into the vent. The pool wall pressure signals are

characterized by pronounced spikes. Vent steam mass flux into the pool, pool temperature, and vent flow air content are known to be important factors affecting the steam condensation process and, thus, the CO-to-chugging transition.

All of the 4TCO test data (Reference 1) were examined and the blowdown conditions at the time of wetting\* of the vent exit level probe noted. Level probe wetting was taken as indication of the start of chugging. In all of the 3.82-inch break tests, the level probe did not wet until the end of the blowdown, and therefore, these data were not included in defining the transition. Vent steam mass flux values inferred from the venturi blowdown flow rate measurements at the time when the level probe started wetting were plotted versus the bulk pool temperature. The observed data were bounded to define a minimum mass flux as a function of pool temperature below which CO evidently could not occur. The solid line in Figure 2-8 was established as the lower bound steam mass flux for CO-to-chugging transition.

#### 2.2.1.2 Mark II Plant Conditions at ADS

Mark II plant conditions (vent steam mass flux and bulk pool temperature) at the time of ADS actuation were calculated for a spectrum of liquid break sizes with potential for CO combination with ADS.

The calculation of plant conditions was performed in two steps:

1. Calculating the break flow rate (mass, enthalpy) from the reactor pressure vessel and the time when ADS actuates after the break occurs. The assumptions/conditions used in the analysis are listed in Table 2-2. These assumptions/conditions will maximize the vent steam mass flux at ADS actuation.
2. Calculating the transient vent flow rate and pool thermodynamic conditions by using break flow data (obtained in Step 1) and plant containment design data. Vent flow into the pool is based on

---

\*Wetting of the level probe confirms water re-entry into the vent.

drywell-to-wetwell pressure difference, and pool temperature is based on integration of the wetwell pool mass and energy.

### 2.2.1.3 CO Conditions Comparison with ADS Conditions

In determining if the CO phenomena can occur simultaneously with ADS actuation the plant ADS conditions, obtained as described in Subparagraph 2.2.1.2, were compared with the CO-to-chugging transition conditions. A comparison of Mark II maximum mass flux values at ADS versus CO-to-chugging transition conditions is shown in Figure 2-9. The conclusion from this figure is that CO can occur simultaneously with ADS actuation; therefore, the CO plus ADS load combination should be evaluated.

### 2.2.2 Criteria for Selection of 4TCO Data

The 4TCO test data show that the CO load magnitude (rms value) is significantly lower at low vent steam mass flux values. Therefore, the low vent steam mass flux values calculated at the time of ADS actuation will produce a CO load which will be significantly lower than the basic CO load for the Mark II plant. Thus, it is appropriate to define a second more representative CO load for combination with the ADS load.

In defining this second CO load to combine with the ADS load, all 4TCO data were screened to determine which data remained applicable for combining with ADS. Results of the data screening revealed that the 2.125-inch liquid break tests were appropriate for consideration. This is the smallest break size ( $\approx 0.025 \text{ ft}^2$  per vent) tested in 4TCO. This break size is substantially higher than the range of plant break sizes (0.013 to 0.021  $\text{ft}^2$  per vent) that produced maximum vent steam mass flux conditions at ADS actuation. Since the 4TCO test data show that for the small breaks tested the total rms pressure values (at the pool bottom center) decreases with a decrease in break size (Reference 1), the 2.125-inch liquid breaks were taken as a conservative data base for the CO load for combination with ADS.



In the break sizes analyzed that would result in ADS actuation, the highest calculated vent steam mass flux at ADS actuation for all Mark II plants ranged from approximately 3 to 5 lbm/sec-ft<sup>2</sup>. As an added margin, a vent steam mass flux of 6 lbm/sec-ft<sup>2</sup> was taken as the upper bound value for vent steam mass flux at which Mark II plants can experience ADS actuation.

### 2.2.3 Description of Data Selected

The CO time periods in the 2.125-inch liquid break tests with vent steam mass flux less than 6 lbm/sec-ft<sup>2</sup> are to be used for the CO load for combination with ADS. A list of these CO time periods is given in Table 2-1. Run 15, a 2.125-inch liquid break, is not included because the CO-to-chugging transition occurred at a mass flux above 6 lbm/sec-ft<sup>2</sup>. Test data obtained after 59 seconds in Runs 13 and 14 were not included in the CO load because chugging started at 59 seconds. All 4TCO data which meets the criteria presented in Paragraph 2.2.2 has been used for the CO load for combination with ADS. Therefore, no analysis to assure that the selected time periods were bounding on a power by frequency basis (PSDs) was required.

## 2.3 APPLICATION PROCEDURE

### 2.3.1 Spatial Distribution of Applied Pressure

During the CO period of the blowdown transient the suppression pool wall and drywell are subjected to dynamic pressure loading. The evaluation of 4TCO test boundary pressures from CO showed that the bottom of the pool experienced the highest dynamic pressure magnitudes. The free surface boundary of the pool, by definition, will experience no dynamic pressure loading.

In evaluating the plant structural response to CO loading, the 4TCO pressure time histories corresponding to the time intervals listed in Table 2-1 are to be applied directly as rigid wall loads to the containment structural model. The 4TCO suppression pool BCP time history is applied uniformly over the entire plant suppression pool boundary below the exit of the vent and is linearly attenuated to zero at the suppression pool surface from the vent exit



elevation. Figure 2-10 shows a detailed spatial distribution of the pressure loading on the suppression pool. The drywell pressure time histories for the time periods defined in Table 2-1 are simultaneously applied uniformly throughout the drywell.

### 2.3.2 Conditions for Load Cases

As discussed and noted in the previous paragraphs, at certain conditions of vent steam mass flux and bulk pool temperature the steam condensation process in the suppression pool shows transition from CO to chugging. Figure 2-8 shows such a transition. The basic CO load should be considered as applicable for all Mark II LOCA conditions following pool swell where plant system performance calculations show vent steam mass flux and pool temperature conditions that are within the CO region as shown in Figure 2-8. For the small break and low mass flux conditions established earlier (Subsection 2. . as being representative of conditions at ADS actuation, the lower CO load is applicable for combination with ADS. Figures 2-11 and 2-12 show the range of tested conditions for the basic CO load and CO load with ADS, respectively.

Table 2-1

4TCO TIME PERIODS FOR BASIC CO LOAD AND CO LOAD WITH ADS

Basic CO Load

<u>Run Number</u>	<u>Time (sec)</u>
3	13 to 15
4	10 to 12
5	19 to 21
8	5 to 7
9	10 to 23
10	28 to 30
12	21 to 25
14	25 to 31
15	31 to 48
22	13 to 21
23	5 to 7
24	12 to 14
25	32 to 42
26	16 to 24, 32 to 36
27	16 to 34
28	17 to 19

CO Load with ADS

<u>Run Number</u>	<u>Time (sec)</u>
13	50 to 59
14	50 to 59

Table 2-2

## BASES AND ASSUMPTIONS FOR THE ADS EVENT

1. Break in recirculation line.
2. Initial water level at normal level.
3. MSIV closure on low-water level.
4. ADS activated on high drywell pressure and low-low-water level.
5. SCRAM on water level signal.
6. Power level at 102 percent rated.
7. ADS delay = 105 sec (nominal delay time)
- \*8. With feedwater and without feedwater.
9. High pressure ECCS systems (HPCI/HPCS) fail. Low pressure systems (LPCI/LPCS) available.
10. Homogeneous Equilibrium Model (HEM) for break flow rate calculations.

---

\*In cases with feedwater, feedwater is available up to two minutes for plants with turbine-driven feedwater pumps, and full continuous flow in plants with motor-driven feedwater pumps. In cases without feedwater, feedwater flow stops at time  $t=0$ .

The following Figures are GENERAL ELECTRIC COMPANY PROPRIETARY and have been removed from this document in their entirety.

- 2-1 Envelope of PSD Values Observed for CO in 4TCO Tests
- 2-2 Wetwell Bottom Center Pressure Time History, 4TCO Run 15, 39 to 41 Seconds
- 2-3 Drywell Pressure Time History, 4TCO Run 15, 39 to 41 Seconds
- 2-4 Wetwell Bottom Center Pressure Time History, 4TCO Run 22, 13 to 15 Seconds
- 2-5 Drywell Pressure Time History, 4TCO Run 22, 13 to 15 Seconds
- 2-6 PSD - Wetwell Bottom Center Pressure for 4TCO Run 15, 39 to 41 Seconds
- 2-7 PSD - Wetwell Bottom Center Pressure for 4TCO Run 22, 13 to 15 Seconds
- 2-8 Mass Flux and Bulk Pool Temperature at CO-to-Chugging Transition in 4TCO Runs
- 2-9 Mark II Maximum Mass Flux at ADS versus CO-to-Chugging Transition in 4TCO Tests

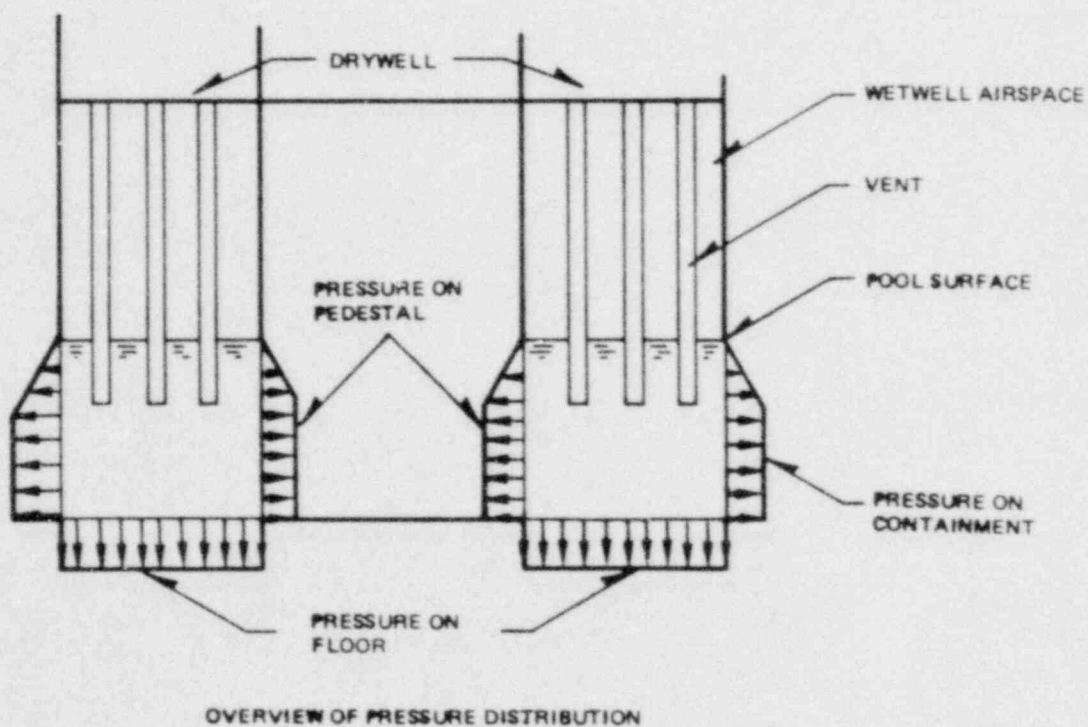
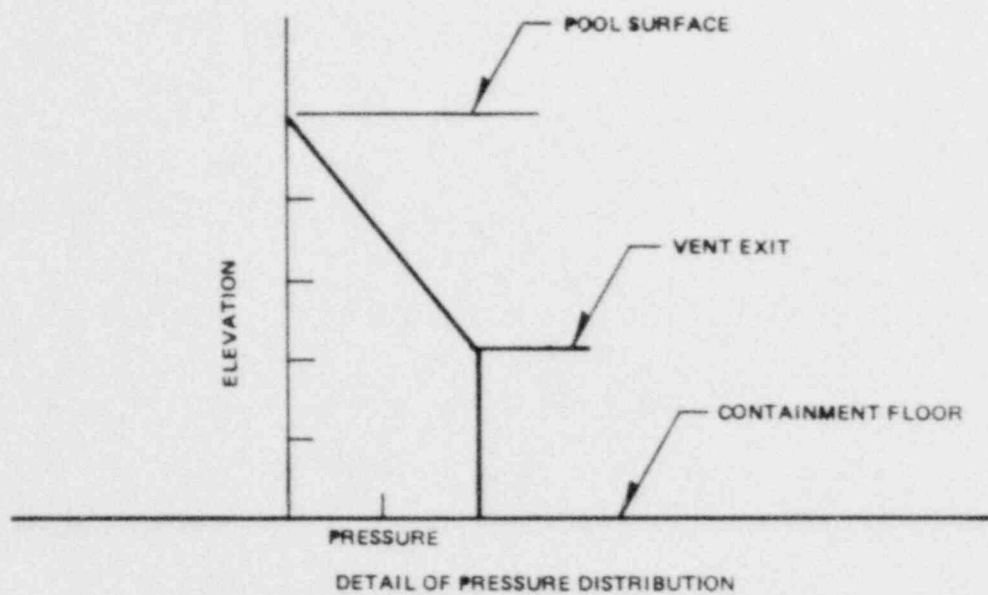


Figure 2-10. Spatial Distribution of CO Load

The following Figures are GENERAL ELECTRIC COMPANY PROPRIETARY  
and have been removed from this document in their entirety.

- 2-11 Basic CO Load - Range of Conditions
- 2-12 CO Load with ADS - Range of Conditions



### 3. JUSTIFICATION OF LOAD DEFINITION

#### 3.1 COMPARISON OF MARK II AND 4TCO BLOWDOWN CONDITIONS

Vent steam mass flux, pool temperature and vent air content are recognized as key parameters which determine the magnitude of the CO load. At a given vent steam mass flux, higher pool temperature and lower vent air content values are expected to produce higher CO loads. The 4TCO test matrix was designed to bound the Final Safety Analysis Report (FSAR) calculated values of these key CO parameters for Mark II plants. Appendix I of the 4TCO final test report (Reference 1) contains details of the basis and approach employed in designing the 4TCO test matrix.

The plant FSAR calculations employ the slip flow model (SFM) for the break flow calculations. However, the SFM has been demonstrated to overpredict the critical flow rates for the liquid breaks, whereas the homogeneous equilibrium model (HEM) provides more accurate blowdown flow rates than the SFM (Reference 3). Considering that break flow governs the vent flow conditions, the 4TCO versus Mark II plant conditions comparison was conducted using the HEM. This evaluation involved (1) establishment of a method, using 4TCO test measurements as the reference, to obtain best-estimate predictions for Mark II plants and 4TCO, (2) calculating best-estimate predictions for Mark II plants and 4TCO test runs using the same method with appropriate initial conditions and design input data, and (3) comparing Mark II plant and 4TCO blowdown conditions. Details of this evaluation are presented in the following paragraphs.

##### 3.1.1 Methodology for Best-Estimate Predictions

In this evaluation only liquid break cases (recirculation line break for Mark II plants and bounding runs for 4TCO) were analyzed because steam breaks produce much lower CO loads than liquid breaks. 4TCO test data and other full-scale CO test data have confirmed this trend.

The appropriateness of the use of the HEM blowdown model for obtaining best-estimate predictions was checked by comparing the 4TCO predicted values (using both HEM and SFM) against the measured values. Input initial conditions for the 4TCO predictions were inferred from the test data.

Figures 3-1 through 3-3 show a comparison of measured versus predicted values for steam generator pressure as a function of time. Since the 4TCO steam generator is a flash boiler with no mass or energy addition during the course of a blowdown, the demonstrated ability to predict the steam generator pressure indicates the calculated blowdown flow rates are also correct. Figures 3-4 through 3-6 show a comparison of measured versus predicted values for vent air content. The good correlation between predicted and measured air content in the vent flow rate shows that the vent flow calculations are also accurate. A comparison of vent steam mass flux was not possible because this parameter was not measured in the 4TCO tests. These comparisons show that the HEM calculation provides good agreement with the measured values and is appropriate for this evaluation.

### 3.1.2 Mark II and 4TCO Blowdown Calculations

Using the established method of calculation the best-estimate predictions of blowdown conditions for Mark II plants and 4TCO test runs were generated. The vent blowdown conditions with a recirculation line break were calculated for all Mark II plants. In these calculations plant unique initial conditions and geometry data (consistent with FSAR calculations) were input, except that a higher value of initial relative humidity in the drywell was used (0.55 as opposed to a value of 0.2 used in FSAR calculations). This higher value which is an upper bound of the range during plant normal operating conditions is expected to produce conservatively low values for plant vent air content.

Figure 3-7 shows calculated blowdown vent steam mass flux versus bulk pool temperature for all Mark II plants. The initial pool temperature values used in these calculations were the maximum operating pool temperature from the technical specification for each plant. This will provide an upper bound value of the pool temperature at a given vent steam mass flux value. Similarly,

Figure 3-8 shows calculated vent steam mass flux versus vent air content (% air by mass in steam-air mixture) values for all Mark II plants. The vent blowdown conditions for the 4TCO runs which have bounding values for these conditions were calculated. Input data for initial conditions, including initial relative humidity in the drywell, were inferred from the test data. Figures 3-9 and 3-10 show calculated 4TCO blowdown values similar to those obtained for Mark II plants.

### 3.1.3 Mark II versus 4TCO Conditions Comparison

Figures 3-11 and 3-12 show a comparison between Mark II plant and 4TCO blowdown conditions on maps of vent steam mass flux versus bulk pool temperature and vent steam mass flux versus vent air content, respectively.

Figure 3-11 shows that the 4TCO test conditions for pool temperature and vent steam mass flux fully bound Mark II plant conditions. At any vent steam mass flux value, the 4TCO tested temperature is significantly higher than the maximum pool temperature expected for all Mark II plants.

Figure 3-12 shows that the 4TCO tested conditions provide bounding vent air content values. At any given vent air content value, the 4TCO tested vent steam mass flux values cover the range and significantly exceed the Mark II calculated values.

Based on the above comparisons, the conclusion is that the 4TCO test matrix bounds all Mark II plant blowdown conditions and provides a conservative data base for Mark II CO load definition.

### 3.1.4 Plant Unique Adjustments for Pool Temperature

Figure 3-11 shows that the 4TCO pool temperature values during CO are conservatively high compared to the calculated pool temperatures for the Mark II plants. The non-representative high temperature 4TCO data was eliminated in developing the LaSalle CO load definition. The LaSalle approach, described in Appendix B, resulted in a conservative CO load definition for

LaSalle. This same approach may be used for other Mark II plants, if desired, but the cutoff temperature and resultant data base may be different than those used for LaSalle.

### 3.2 COMPARISON OF MARK II CONTAINMENT AND 4TCO GEOMETRIES

The 4TCO test facility, which is a full-scale single vent representation of a prototypical Mark II design, was designed to produce test data to define the CO load magnitude for Mark II plants. In establishing key dimensions of the 4TCO test facility the geometric parameters considered to be significant to the CO phenomena were examined for all Mark II plants. Table 3-1 shows a comparison between 4TCO and Mark II values for these parameters. The significance of each design parameter as related to the CO phenomena is discussed in the following paragraphs. The 4TCO geometry is shown to be representative or bounding for establishing the data base for the Mark II CO load definition.

#### 3.2.1 Break Area Per Vent

The break area per vent is a key parameter in establishing the vent flow rate which has been shown to be an important variable in determining the CO load amplitude. The 4TCO range of break sizes, as given in Table 3-1, bounds all Mark II plants on a break area per vent basis.

#### 3.2.2 Vent Length

The vent length is expected to influence the frequency content of the suppression pool wall loads by changing the vent acoustic resonant frequencies. The 4TCO vent length given in Table 3-1 is representative of the Mark II plants.

### 3.2.3 Vent Submergence

Vent submergence indirectly affects the CO load by affecting both local and bulk pool temperature values and changing the acoustic resonant frequencies for the pool which influence the CO load frequency content. The 4TCO tested vent submergence values given in Table 3-1 cover the range of Mark II plant submergence.

### 3.2.4 Vent to Pool Bottom Clearances

This parameter is expected to affect the acoustic resonant frequencies for the pool which influence the CO frequency content. The 4TCO design value for vent to pool bottom clearance given in Table 3-1 is representative of all Mark II plant values.

### 3.2.5 Pool Area-to-Vent Area Ratio

Based on earlier experimental studies (Reference 4), the containment boundary load is expected to decrease with the pool-to-vent area ratio. The pool area-to-vent area ratio for the 4TCO facility is low compared to the ratio for the Mark II plants, as shown in Table 3-1. This low value is expected to result in a bounding CO load from the 4TCO tests.

### 3.2.6 Drywell Volume Per Vent

The drywell volume per vent affects the vent steam mass flux and vent air content. Reducing the drywell volume results in increased vent steam flow rates and decreased vent air content during the CO time period. Since either increasing the vent steam flow rate or decreasing the vent air content results in higher amplitude CO, the CO amplitude is expected to increase as the drywell volume per vent is decreased. The 4TCO drywell volume is shown in Table 3-1 to be small compared to the Mark II plant values. This small 4TCO drywell volume per vent is expected to result in 4TCO values for CO wall pressures which are conservative for application to Mark II plants.



### 3.2.7 Wetwell Airspace Volume-to-Drywell Volume Ratio

This parameter is expected to affect the CO load indirectly by influencing the drywell air clearing transient and the degree of subcooling in the vent exit region. The 4TCO value given in Table 3-1 for this parameter is representative of the range for Mark II plants.

### 3.2.8 Pool Mass Per Vent

For a given blowdown into the pool, a smaller pool mass (per vent) will result in periods of higher pool temperature at the same vent flow than in larger pools. Higher pool temperatures tend to increase the CO load magnitude. The 4TCO tested range of pool mass per vent given in Table 3-1 is low compared to the Mark II range. This is expected to provide conservative CO test data for application to Mark II plants.

### 3.2.9 Plant Unique Adjustments for Pool Geometry

The previous discussion shows that the 4TCO pool geometry is a conservative representation of the Mark II plant geometries. Mark II plants vary somewhat in pool size and number of vents. As a result, the 4TCO loads contain a geometric conservatism which is unique to each plant. A geometric load reduction factor was included in the LaSalle CO load definition. The methodology, used to determine this pool geometry factor for the LaSalle CO load as presented in Appendix B, may be applied to other plants, if desired.

## 3.3 4TCO COMPARISON WITH MULTIVENT DATA

The objective of this discussion is to confirm that the single vent 4TCO data is conservative for application to the multivent Mark II geometry. The confirmation study presented here is based on comparisons of pressure



measurements in the 4TCO facility with measurements from the JAERI facility. First, all the initial test conditions of the 4TCO and JAERI test runs were compared. Results showed that while there are no exact matches of initial values of all test parameters between 4TCO and JAERI, there are several 4TCO runs which are similar to JAERI Test 1101. JAERI Test 1101 was selected for comparison because it resulted in the maximum rms pressure during CO for any available JAERI test with conditions representative of expected Mark II blowdown conditions. The initial conditions for these tests are shown in Table 3-2. The 4TCO Runs 2, 5 and 7 are seen as having all conditions close to that of JAERI Test 1101, except that the JAERI test includes a vent riser. The 4TCO Runs 26 and 28 include the vent riser, but they have a higher initial pool temperature than JAERI Test 1101.

The preceding 4TCO runs all had a 3.00-inch diameter venturi. This is equivalent to the JAERI Test 1101 200-mm break on a break area per vent basis. However, the JAERI Test 1101 blowdown flow rates are somewhat reduced by increased fluid friction losses in the blowdown line to the venturi. This in effect is equivalent to a smaller JAERI venturi area. 4TCO Run 25 used a 2.50-inch diameter venturi which is 29 percent smaller on a break area per vent basis than JAERI Test 1101. This break size is expected to result in low blowdown flow rates compared to JAERI Test 1101. However, 4TCO Run 25 is also compared with JAERI Test 1101 to insure that no bias has been introduced into the comparison by using 3.00-inch 4TCO tests which may have high flow rate values compared with the 200-mm JAERI test.

Figure 3-13 shows the observed bulk pool temperature histories for 4TCO Runs 2 and 5 and JAERI Test 1101. The JAERI temperature history is an unweighted average of 16 temperature sensors distributed throughout the pool, while the 4TCO temperature histories are an average of 11 pool temperature sensors weighted on a representative pool volume basis. JAERI Test 1101 is within 10°F of both 4TCO runs throughout the CO period. The bulk pool temperature histories for 4TCO Runs 25, 26 and 28 are not comparable to that of JAERI Test 1101 due to the difference in initial pool temperature.

### 3.3.1 Comparison of JAERI and 4TCO Suppression Pool Pressures

Figure 3-14 shows the rms histories for two sensors on the bottom of the JAERI facility (WWPF-101 and WWPF-104) during the CO period in JAERI Test 1101. The rms histories of other pool bottom sensors differ little from these. Comparing this figure with the 4TCO rms histories (Figures 3-15, 3-16 and 3-17), each of the six 4TCO pool bottom rms histories are seen to bound both JAERI rms histories throughout the CO time period.

Figures 3-18, 3-19 and 3-20 are bounding PSD plots from the 4TCO tests used for the comparison for the two second time periods of maximum rms power during CO. Figure 3-18 is a bounding PSD for 4TCO Run 2 (25 to 27 seconds), 4TCO Run 5 (11 to 13 seconds) and 4TCO Run 7 (25 to 27 seconds). Similarly Figure 3-19 is a bounding PSD for 4TCO Run 26 (16 to 18 seconds) and 4TCO Run 28 (17 to 19 seconds), and Figure 3-20 is the PSD for 4TCO Run 25 (20 to 22 seconds). Figure 3-21 is a bounding PSD for JAERI Test 1101 using pool bottom sensors WWPF-101 to WWPF-104 and WWPF-107 for a time interval of 15.7 to 24.7 seconds (the PSD values were obtained using approximately 2-second analysis periods). This is the period of maximum rms power during CO for this test. A comparison of these four PSDs show that the JAERI Test 1101 PSD is bounded by all of the 4TCO PSDs at all frequencies. The 4TCO PSDs exceed the JAERI Test 1101 PSD by a large margin, particularly at frequencies below 5 Hz and above 13 Hz.

Attention is turned now to whether the difference between the 4TCO rms signal strength and the rms signal strength in JAERI is due entirely to a multivalent effect or to a difference in source strength. Table 3-3 summarizes the rms values at vent exit and pool bottom in the 4TCO and JAERI facilities, which have been averaged in time over approximately the strongest 8 seconds of CO for each run. The JAERI values were also averaged spatially.

The average pool bottom rms for the 4TCO runs and times specified in Table 3-3 is compared to an average value for JAERI Test 1101. The ratio of these two values gives a comparative 4TCO pool bottom signal strength relative to JAERI.

The average 4TCO vent exit rms is compared to a value of JAERI. The ratio of these values gives a comparative 4TCO vent exit signal strength relative to JAERI. Thus there is essentially no difference in vent exit signal strength under comparable conditions. Nearly all the reduction of pool bottom signal is due to a multivalent effect.

### 3.3.2 Comparison of JAERI and 4TCO Drywell Pressures

Figure 3-22 shows the bounding PSD values of the JAERI drywell pressure measurement from two second analysis blocks during the CO period in JAERI Test 1101. The bounding PSD values of drywell acoustic pressure from two seconds analysis blocks for 4TCO Runs 2, 5, 7, 25, 26 and 28 are also shown in this figure.

The PSD values at all frequencies for 4TCO selected runs, as shown in Figure 3-22, are significantly higher than the PSD values obtained from JAERI Test 1101, particularly at frequencies around 1 Hz. This comparison shows that the single vent 4TCO drywell pressure oscillations are large compared with the JAERI multivalent values which supports the conclusion that the 4TCO values are conservative for application to the Mark II multivalent geometry.

### 3.4 4TCO FLUID-STRUCTURE INTERACTION EVALUATIONS

The results of the 4TCO FSI evaluations summarized here support the following conclusions:

- a. Measured pressure amplitudes at low frequencies (<30 Hz) are essentially unaltered by boundary flexibility.
- b. Measured pressure amplitudes at higher frequencies (>30 Hz) are conservative relative to those which would have occurred in a rigid facility.

These conclusions are the basis for using the measured wall pressures without modification for evaluation of plant structural responses.

References 5 and 6 have shown that one potential FSI effect is a shift in the frequencies of the 4TCO pool acoustic modes induced by flexibility of the steel boundary. The present study indicates that this effect is not significant for the 4TCO wall pressures. A second potential FSI effect is the introduction of structural resonances. The structural modes examined included (1) bouncing of the entire facility on its concrete/soil foundation, (2) vibration of the baseplate, and (3) vibration of the sidewall. Calculations performed in support of this study show that the net effect of these modes is to produce more high-frequency response in the pressure signals than would be seen in a rigid facility. Therefore, it is conservative to use the measured pressures directly for plant evaluation. Details of the 4TCO FSI evaluation are presented below.

#### 3.4.1 Acoustic Modes

Structural flexibility is known to lower the frequency of pool acoustic modes by effectively decreasing the bulk modulus of the water. Reference 6 has shown that this effect can be predicted by the formula

$$\frac{f}{f_R} = \frac{1}{\sqrt{1 + (BD/Et)}}$$

where

- f = flexible-wall frequency
- f<sub>R</sub> = rigid-wall frequency
- B = fluid bulk modulus
- E = Young's modulus (for steel = 30 x 10<sup>6</sup> psi)
- D = tank diameter (84 inches)
- t = tank thickness (0.625 inch)

The bulk modulus can be expressed as  $\rho C_o^2$  where  $\rho$  is the water density and  $C_o$  is the wave speed. This formula has been used in standard calculations of

the effect of pipe flexibility on wave propagation during waterhammer (see Reference 7, for example). It simply expresses the fact that fluid in a flexible container appears to be more compressible because expansion and contraction of the wall can accommodate volume change.

The wave speed  $C_0$  is very sensitive to small amounts of air entrained in the water (Reference 7). Estimates of the wave speed from the 4TCO data indicate that for most of the load definition time periods the value was less than 1400 fps. This means that the air/water mixture has a very low bulk modulus and the additional effect of steel flexibility is very slight.

It can be shown with the above formula that for wave speeds below 1400 fps the frequency shift of the acoustic modes would be no greater than 6 percent. This effect is too small to produce any significant distortion of the measured wall pressures.

4TCO Run 15 is the only identified 4TCO test with wave speeds in excess of 1400 fps during the CO regime. The inferred values for the load definition time period (31 to 48 seconds) range from 600 fps to 3700 fps. In evaluating the potential effect of wall flexibility for the higher wave speeds observed in 4TCO Run 15 it is important to note that data from the downcomer exit pressure transducer have no significant signal content above 30 Hz. This is clearly illustrated by Figures 3-23 and 3-24 which cover the 30 to 50 second period of 4TCO Run 15. It has been confirmed that this pressure transducer was in the steam throughout this time period. The implication is there are no sustained sinusoidal CO driving frequencies above 30 Hz. Since there are frequencies below 30 Hz in the vent signal it becomes appropriate to treat the potential effect of frequency shifts for suppression pool modes separately for frequencies below and above 30 Hz.

Further examination of 4TCO Run 15 data shows that wall pressures below 30 Hz are not being influenced by wall flexibility. Figures 3-25 and 3-26 show the transfer function (ratio of pressure amplitudes) from the vent exit pressure to the wetwell BCP. It is seen that the amplitude ratio is less than two



for frequencies below 30 Hz. It is concluded that the excitation of suppression pool resonances by vent signals in this frequency range is at most a low-level, broad-band effect which would not be sensitive to moderate shifts in the suppression pool resonant frequencies. It is hypothesized that the conditions at the vent exit during CO inhibit the development of the standing quarter-wave which would be predicted to occur in this frequency range for the 4TCO Run 15 wave speeds.

A possible explanation for the higher frequencies (>30 Hz) which appear in the wall data is that they are 4TCO system responses to impulsive excitation at the vent exit or some other location in the pool. The frequency spectrum of these responses may be altered by tank flexibility but this effect is not considered to be significant for Mark II application. The reason for this is that these are not CO "driver" frequencies. Evidence presented below indicates that the high-frequency end of the wall pressure spectrum is probably being intensified by boundary flexibility. It was not possible within the schedule limitations to attempt a high-frequency FSI correction so this effect is conservatively retained in the wall pressure data.

#### 3.4.2 Facility Bounce Mode

The possibility of a facility bounce mode in which the mass of the 4TCO structure vibrates on its concrete/soil foundation was investigated by examining data from the accelerometer on the baseplate flange. The data, in general, show that there was negligible vertical acceleration of the facility (rms signal strength <0.02g). A typical example, recorded from 16.1 to 18.5 seconds in 4TCO Run 9, is shown in Figure 3-27. Discrete spikes, however, were recorded by the flange accelerometer during some of the time periods included in the load definition. The maximum amplitude was 0.16g at 18 seconds in 4TCO Run 26.

Bottom center pressure and baseplate accelerometer data were examined at the time of the maximum flange acceleration in 4TCO Run 26. The flange acceleration spikes are in phase with the associated pressure spikes, i.e., acceleration



is downward when pressure is positive, and taken by themselves would indicate the possibility of an attenuation of the peak pressure amplitudes. Examination of the baseplate acceleration at the same time, however, shows that it is out of phase with the flange acceleration and BCP signals. The conclusion is that the net effect of the gross vertical motion of the facility and the independent motion of the baseplate was to increase the amplitude of the pressure spikes.

### 3.4.3 Baseplate/Sidewall Vibration

The potential effects of vibration of the 4-inch thick baseplate and the 0.625-inch thick cylindrical sidewall were investigated with a coupled fluid-structure NASTRAN model of the 4TCO facility. In addition to the baseplate, sidewall, and contained water, the model included the effect of the 25-ton drywell mounted on top of the cylindrical tank. Modeling of the baseplate was facilitated by test results presented in Reference 5 which show that the baseplate without water has a fundamental vibration frequency of 190 Hz. This is about 15% below the theoretical value for a clamped circular plate (Reference 8) and was used to justify a clamped edge condition in the NASTRAN model. The model was restricted to axisymmetric deformation. This assumption is supported by data from pressure transducers at different orientations on the tank wall at the same elevation. Figures 3-28 and 3-29 show PSDs of pressure traces from 4TCO Run 15 at two transducer locations separated by 90° at the 12-ft elevation. It is possible that the shell was vibrating non-symmetrically but these data show that such modes, if they occurred, had no effect on measured pressures. The model was based on an incompressible representation of the contained fluid. This was done because (1) the influence of boundary flexibility on acoustic modes is known to be negligible for most of the 4TCO data, (2) the data indicate that the full-depth standing waves which would be predicted by a compressible model are not strongly excited during CO, and (3) modeling the fluid as incompressible would most clearly show the effect of structural resonances. Final verification of the NASTRAN structural model was accomplished by applying measured wall pressures for selected CO time segments and comparing measured and predicted values of sidewall and baseplate strain.

One prediction of the NASTRAN model is the existence of an axisymmetric sidewall vibration mode at a frequency of about 40 Hz. This mode is associated with vertical acceleration of the drywell mass with the cylindrical shell acting as a spring. Poisson's ratio coupling between axial and radial deformation of the cylinder indicates that the mode could be excited by a pressure force acting laterally on the inside surface but it is likely that this will be a small effect because the mode is dominated by axial displacement.

Figure 3-30 shows a frequency response curve obtained from the NASTRAN calculations. This curve shows the BCP amplitude normalized to the rigid-wall value as a function of frequency for a unit harmonic acceleration imposed at the vent exit. The resonance in this transfer function is due mainly to a coupling between the breathing mode of the shell (dry frequency ~800 Hz) and the inertia of the tank water. It is possible there is also a small contribution from the axial mode described above. It is seen that for all frequencies below 60 Hz the effect of structural flexibility is to increase the pressure amplitude.

Evidence of high frequency structural response is also present in transfer function data from 4TCO Run 15. Figure 3-31 shows a distinct peak in the ratio of strain to pressure at the 12-ft elevation at a frequency of about 49 Hz. The fact that the measured frequency is higher than the predicted frequency is possibly explained by the boundary condition imposed at the vent exit for the NASTRAN calculation. In the calculation described above the fluid acceleration was prescribed on the vent exit plane. A similar calculation, except with the pressure prescribed on the vent exit plane, predicts a resonance at 57 Hz. It is not unreasonable to believe that the true vent exit condition is somewhere between these extremes leading to an intermediate frequency for the coupled fluid-sidewall mode.

Further investigation of the coupled response characteristic of the system at high frequency might lead to a quantitative evaluation of the amount by which the high frequency amplitudes are being increased by FSI. It was not possible to do this within the schedule limitations so the measured amplitudes are conservatively retained in the load data.

Table 3-1  
4TCO VERSUS MARK II GEOMETRIC PARAMETERS

Parameter	4TCO	Mark II Range
1. Break Area Per Vent, (ft <sup>2</sup> )	0.025 - 0.080	0.025 - 0.049*
2. Vent Length, (ft)	45.3	36.8 - 51.0
3. Vent Submergence, (ft)	9.0, 11.0, 13.5	9.0 - 12.3
4. Vent to Pool Bottom Clearance, (ft)	11.8	9.0 - 19.0
5. Pool Area-to-Vent Area Ratio	12	14 - 19
6. Drywell Volume Per Vent, (ft <sup>3</sup> )	1910	1970 - 2750
7. Wetwell Airspace Volume-to-Drywell Volume Ratio	0.5 - 0.6	0.5 - 0.7
8. Pool Mass Per Vent, ( $\sim$ lb <sub>m</sub> )	48000 - 59000	54000 - 90000

\*Recirculation line break per vent basis

Table 3-2  
INITIAL CONDITIONS FOR COMPARABLE JAERI AND 4TCO TESTS

Test Facility and Run Number	Break Type	Venturi Diameter (in)	Break Area Per Vent (in <sup>2</sup> )	Vent Exit Submergence (ft)	Initial Bulk Pool Temp (°F)	Vent Riser
JAERI 1101	liquid	7.87	6.96	11.9	86	yes*
4TCO 2	liquid	3.00	7.07	11.0	76	no
4TCO 5	liquid	3.00	7.07	11.0	79	no
4TCO 7	liquid	3.00	7.07	11.0	93	no
4TCO 26	liquid	3.00	7.07	11.0	111	yes
4TCO 28	liquid	3.00	7.07	11.0	110	yes
4TCO 25	liquid	2.50	4.91	11.0	111	yes

\*The vent risers used in the JAERI facility extended 7.6-inches above the drywell floor, while the vent riser used in 4TCO extended 24-inches above the drywell floor. This gives the JAERI drywell approximately 50% of the 4TCO liquid retention capability on the basis of liquid retention volume per vent.

Table 3-3

## AVERAGE RMS PRESSURE VALUES AT VENT EXIT AND POOL BOTTOM

<u>Test Facility and Run Number</u>	<u>Average rms* - psi</u>	
	<u>Vent Exit</u>	<u>Pool Bottom</u>
JAERI 1101		
4TCO 2		
4TCO 5		
4TCO 7		
4TCO 26		
4TCO 28		
4TCO 25		
4TCO Average		

\*The average is taken over the 8-second time period of maximum rms during CO for the 4TCO runs. In the JAERI test the average is taken over the 8-second time period of maximum rms during CO and over two pool bottom sensors WPPF-101 and WPPF-104. Other JAERI pool bottom sensor rms values differ little from these.



The following Figures are GENERAL ELECTRIC COMPANY PROPRIETARY and have been removed from this document in their entirety.

- 3-1 Steam Generator Dome Pressure - Measured versus Predictions - 4TCO Run 3
- 3-2 Steam Generator Dome Pressure - Measured versus Predictions - 4TCO Run 2
- 3-3 Steam Generator Dome Pressure - Measured versus Predictions - 4TCO Run 12
- 3-4 Vent Air Content - Measured versus Prediction - 4TCO Run 8
- 3-5 Vent Air Content - Measured versus Prediction - 4TCO Run 9
- 3-6 Vent Air Content - Measured versus Prediction - 4TCO Run 12
- 3-7 Mark II Plants Calculated Blowdown Conditions - Vent Steam Mass Flux versus Bulk Pool Temperature
- 3-8 Mark II Plants Calculated Blowdown Conditions - Vent Steam Mass Flux versus Vent Air Content
- 3-9 4TCO Calculated Blowdown Conditions - Vent Steam Mass Flux versus Bulk Pool Temperature
- 3-10 4TCO Calculated Blowdown Conditions - Vent Steam Mass Flux versus Vent Air Content
- 3-11 Mark II Plants and 4TCO Comparison on Map of Vent Steam Mass Flux versus Bulk Pool Temperature
- 3-12 Mark II Plants and 4TCO Comparison on Map of Vent Steam Mass Flux versus Vent Air Content
- 3-13 JAERI and 4TCO Bulk Pool Temperature Comparison
- 3-14 Pool Bottom rms Pressure Time Histories, JAERI Test 1101
- 3-15 Pool Bottom rms Pressure Time Histories, 4TCO Runs 2, 5 and 7
- 3-16 Pool Bottom rms Pressure Time Histories, 4TCO Runs 26 and 28
- 3-17 Pool Bottom rms Pressure Time History, 4TCO Run 25
- 3-18 Bounding PSD for 4TCO Runs 2, 5 and 7



The following Figures are GENERAL ELECTRIC COMPANY PROPRIETARY and have been removed from this document in their entirety.

- 3-19 Bounding PSD for 4TCO Runs 26 and 28
- 3-20 Bounding PSD for 4TCO Run 25
- 3-21 Bounding PSD for JAERI Test 1101
- 3-22 Comparison of Bounding Drywell Pressure PSD for Comparable 4TCO Runs with JAERI Test 1101
- 3-23 PSD of Downcomer Exit Pressure for 4TCO Run 15, 30 to 40 Second Period
- 3-24 PSD of Downcomer Exit Pressure for 4TCO Run 15, 40 to 50 Second Period
- 3-25 Ratio of Bottom Center to Downcomer Exit Pressure Amplitude for 4TCO Run 15, 30 to 40 Second Period
- 3-26 Ratio of Bottom Center to Downcomer Exit Pressure Amplitude for 4TCO Run 15, 40 to 50 Second Period
- 3-27 Baseplate Flange Accelerometer Reading for 4TCO Run 9, 16 to 18 Second Period
- 3-28 PSD of Pressure at 12-ft Elevation, 315° Orientation for 4TCO Run 15, 40 to 42 Second Period
- 3-29 PSD of Pressure at 12-ft Elevation, 45° Orientation for 4TCO Run 15, 40 to 42 Second Period
- 3-30 Calculated Ratio of Flexible to Rigid Wall Pressure Amplitude for Unit Harmonic Acceleration at Vent Exit
- 3-31 Ratio of Hoop Strain to Pressure Amplitude at 12-ft Elevation for 4TCO Run 15, 40 to 50 Second Period

4. CONCLUSION

Two load cases have been developed for a generic Mark II CO load definition based on direct application of 4TCO pressure measurements. The 4TCO data have been shown to be conservative for this application by:

- a. Comparing 4TCO test conditions to Mark II blowdown conditions.
- b. Comparing 4TCO geometry values to corresponding Mark II values.
- c. Comparing 4TCO single vent drywell and suppression pool pressure values with JAERI multivent values.
- d. Demonstrating that 4TCO wall pressure values would be less if the facility were absolutely rigid.

In addition, the 4TCO data selected for the load definition bound all CO data from the 4TCO tests on either a PSD or ARS basis. Therefore, it is concluded that the generic load definition presented here is adequately conservative for application to the Mark II plants.

REFERENCES

1. "4T Condensation Oscillation (4TCO) Test Program Final Test Report,"  
NEDO-24811, July 1980
2. "Mark II Containment Dynamic Forcing Function Information Report,"  
NEDO-21061, Revision 3, June 1978
3. "Maximum Discharge Rate of Liquid-Vapor Mixtures from Vessels,"  
NEDO-21052, September 1975
4. "Comparison of Single and Multivent Chugging at Two Scales,"  
NEDO-24781-1, January 1980
5. "Summary of 4T Fluid-Structures Interaction Studies,"  
NEDO-23710, September 1978
6. "Mark II Improved Chugging Methodology,"  
NEDO-24822, June 1980
7. E. B. Wylie and V. L. Streeter, "Fluid Transients," McGraw-Hill, 1978.
8. A. W. Leissa, "Vibration of Plates," NASA SP-160, 1969.

## APPENDIX A

AMPLIFIED-RESPONSE-SPECTRA CONFIRMATION OF  
SELECTED TIME PERIODS

As described in Paragraph 2.1.2, the BCP time histories used for the basic CO load definition were selected to bound the maximum PSD values observed throughout the CO periods. Including all time periods which yielded the maximum PSD values assures that all signals with maximum power at a given frequency have been included. To assure that adequate signal duration was maintained an analysis which could reflect the response buildup in time to this loading was required.

The form of an oscillatory excitation can be characterized by three parameters, amplitude, frequency content, and damping. An evaluation criterion that combines all three parameters is the response spectrum. When the physical nature of an oscillatory excitation is that of an acceleration time history acting at the support of a structure, an acceleration-response-spectrum is a traditional evaluation criterion. In the case where the oscillatory excitation is a pressure time variation, a pressure-response-spectrum (PRS) is often used as an evaluation criterion. A PRS is generated by simply substituting a pressure time variation for the acceleration time history in a traditional acceleration response spectra calculational routine. The response evaluations presented here are based on the PRS approach to compute the amplified pressure responses. Note that these evaluations are not indicative of the structural response for any particular plant structure, but are general characterizations of the response for a series of single-degree-of-freedom systems covering the range of frequencies of interest subjected to an input pressure time history.

The PRS for each of the BCP time histories selected for the basic CO load definition were calculated. The envelope of these PRS was compared with the envelope of the PRS developed for the entire CO time periods of these selected runs (Table A-1). Figures A-1 through A-17 give the PRS for the time histories selected for CO load definition. The envelope of these PRS is presented in Figure A-18. Figure A-19 shows the envelope of the PRS developed for the entire CO

time periods. Figure A-20 gives the comparison of these two envelopes. Figure A-20 shows that the envelope of the responses for the time periods selected have very small differences from the envelope covering the entire CO time periods. The time periods provided in Table 2-1 are considered to be long enough to assure response buildup equivalent to that if the entire CO periods were used for load definition.

Table A-1  
CO DURATION FOR 4TCO RUNS USED FOR BASIC CO LOAD

<u>Run Number</u>	<u>CO Duration (sec)</u>
3	5-29
4	5-29
5	5-38
8	5-28
9	5-38
10	5-41
12	5-48
14	5-59
15	5-50
22	5-32
23	5-28
24	5-30
25	5-29, 32-44
26	5-24, 29-37
27	5-40
28	5-36



All Figures of this Appendix are GENERAL ELECTRIC COMPANY PROPRIETARY and have been removed from this document in their entirety.

## APPENDIX B

## PLANT UNIQUE ASSESSMENT OF THE 4TCO DATA FOR LASALLE

The test facility geometry was designed to produce a bounding response to the blowdowns which simulate the LOCA to make certain that data from the 4TCO tests are representative of all Mark II plants. Similarly, the range of test parameters investigated in the 4TCO blowdowns bounds the range for all Mark II plants. Because of the much smaller pool area per vent in the 4T facility, the loads measured in the 4TCO test series are higher than would be expected for a geometry with a pool volume per vent representative of LaSalle. Similarly, the range of pool temperatures tested in the 4TCO series exceeds the range of pool temperatures expected in the LaSalle pool. This appendix discusses the plant unique assessment of the 4TCO data to account for the LaSalle pool geometry and range of pool temperature.

## B.1 POOL SIZE EFFECT

In establishing the condensation oscillation load for the assessment of the LaSalle containment, bounding wall pressures measured in the 4TCO tests can be reduced by 20% because of the larger pool size in the LaSalle containment. The ratio of pool area-to-vent area for the 4TCO tests is 12 which represents a bounding pool area-to-vent area ratio for the Mark II plants. The pool area-to-vent area ratio for LaSalle is 16, one third more than the 4T test facility. In terms of pool volume, LaSalle has 75% more pool volume per vent than the 4T. The effect of this larger pool size is to reduce the loads on the containment boundary.

The pool size effect has been demonstrated both experimentally and with analysis. Pool size was one of the parameters studied in the Mark II multi-vent test program (Reference B1). In a special series of experiments, chugging loads were measured for a 1/10 scale vent chugging in various size wetwells. Figures B-1 and B-2 show the decrease of the measured mean peak overpressure as a function of pool size. The trend in these data, which covers a wide range of steam mass flux and two different pool temperatures, follows closely the  $(1/D_w^2)$  curve which is representative of the variation in pool volume.

This experimental result is not unexpected and a similar trend has been predicted with the Mark II chugging model (Reference B-2). This model represents the pool as an acoustic medium. Flow sources at the location of the vent exits are used to represent the condensation events which produce a load on the containment boundary. The effect of pool volume predicted with this model is dependent on the load duration or frequency content and the acoustic frequencies of the containment pool. For condensation oscillation loads, the significant load amplitudes are in the frequency range below 10 to 15 Hz and for this frequency range, the pool volume effect can be clearly demonstrated. Figure B-3 shows the response to a sinusoidal forcing function applied in-phase at all vents calculated using the model from Reference B-2 for the LaSalle containment, compared to the response of the 4T to the same forcing function. The 4T calculations were made using the actual 4T pool area and the same vent submergence and clearance as LaSalle. The LaSalle pool boundary pressure amplitude can be seen to be less than 80% of the 4TCO pool response over a wide range of pool acoustic velocities and forcing function frequencies. Based both on the experimental results from the multivent test program and analytical studies with the model described in Reference B-2, the load reduction for the larger LaSalle pool is justified.

## B.2 POOL TEMPERATURE EFFECT

All but one of the 4TCO blowdowns were conducted with either a cold initial pool temperature ( $\sim 70^{\circ}\text{F}$ ) or a hot initial pool temperature ( $\sim 110^{\circ}\text{F}$ ) to investigate effects of pool temperature on condensation loads. It was generally found that the large liquid break tests which were initiated with a high initial pool temperature exhibited larger condensation oscillation load amplitudes. However, because of the relatively small pool volume, the pool temperature rise observed in the 4TCO tests, particularly those without the vent riser, exceeded the final pool temperature expected in LaSalle. In restricting the data base to conditions closer to those typical of LaSalle, temperature limits were established to define bounding portions of the 4TCO data to use. Operating limits for LaSalle require the suppression pool temperature not exceed  $100^{\circ}\text{F}$ . The total temperature rise shown in the LaSalle FSAR is  $35^{\circ}\text{F}$  following a Design Basis Accident

(DBA) size recirculation line break and 30°F for a main steam line break. An additional 5°F margin was added to this temperature rise to establish temperature limits of 140°F for the 4TCO liquid breaks and 135°F for the steam breaks. In terms of bulk temperature rise, all of the 4TCO steam blowdowns and those liquid breaks with an initial pool temperature of 70°F reach a final pool temperature within the range of pool temperatures that could be expected in LaSalle. However, the 4TCO liquid blowdowns with high initial pool temperatures exceed these limits during their blowdowns. In these tests, only the data taken up to the point where the bulk pool temperature was equal to or less than the temperature limits were used for the LaSalle CO load definition.

These temperature limits are conservative and bounding for LaSalle for two reasons. First, the limits are based on the total LaSalle pool temperature rise and at the time in the blowdown when the condensation oscillation loads occur, the energy dump to the pool is only 2/3 to 3/4 of the total energy dump. Second, the 5°F margin represents an additional 15% margin in energy dump to the pool, nearly  $45 \times 10^6$  BTUs.

Figure B-4 shows the LaSalle pool temperature rise taken from the FSAR, for the main steam line, the DBA recirculation line break and that break for LaSalle which is equivalent to the smallest break in the 4TCO test series. Also shown are bulk temperature rise for tests with hot and cold pool both with and without the vent riser. The differences between the LaSalle pool heatup and the 4TCO pool heatup can be clearly seen.

Although the majority of the 4TCO blowdown data which is used for the condensation oscillation load are from the hot pool tests, the elimination of those parts of the blowdowns with pool temperatures which are outside the range expected for LaSalle represents only a small portion of the data base.

All Figures of this Appendix are GENERAL ELECTRIC COMPANY PROPRIETARY  
and have been removed from this document in their entirety.

NEDO-24288

APPENDIX B

REFERENCES

- B1. "Comparison of Single and Multivalent Chugging at Two Scales,"  
NEDE-24781-1-P, January 1980.
- B2. "Mark II Improved Chugging Methodology," NEDE-24822-P, May 1980.